The Role of Internal Rotational Barriers in Polymer Melt Chain Dynamics

S. Krushev and W. Paul*

Institut für Physik, Johannes-Gutenberg-Universität, Staudingerweg 7, D-55099 Mainz, Germany

G. D. Smith

Department of Materials Science and Engineering and Department of Chemical and Fuels Engineering, University of Utah, 122 S. Central Campus Dr. Rm. 304, Salt Lake City, Utah 84112

Received September 5, 2001; Revised Manuscript Received February 20, 2002

ABSTRACT: We present molecular dynamics simulations on 1,4-polybutadiene comparing the dynamics of melt chains between chemically realistic models and a freely rotating chain version of one of the models. These models exhibit the same liquid structure, as measured by the structure factor, and meso- to large-scale chain structure, as measured by the Rouse-mode amplitudes. We show that in this case the Rouse-like chain dynamics as observable in the momentum transfer range of neutron spin-echo experiments is the same for the chains with and without torsion barriers. Our results bear on a recent comparative neutron spin-echo study of the chain dynamics of two polymers with similar chain structure which revealed a strong difference of the dynamics as quantified by the level of agreement of the scattering data with the Rouse model predictions.

I. Introduction

The universal nature of large-scale polymer properties has motivated a long-standing and successful investigation of these properties using coarse-grained polymer models such as lattice random walks and bead−spring type models.[1] From the coarse-grained point of view the chemical structure determines prefactors of universal laws, e.g., the statistical segment length σ linking the mean-squared end-to-end distance of melt chains to the number of statistical segments N_σ per chain ($R_e^2 = \sigma^2 N_\sigma$) or the monomer friction coefficient ζ linking the self-diffusion coefficient of unentangled chains to the chain length N ($D = k_B T/\zeta N$, $N \propto N_\sigma$).

From the point of view of chemically realistic models, an accurate quantitative description of the static and dynamic properties of a specific polymer can only be obtained through a judicious determination of force field parameters for bonded and nonbonded interactions.[2−4] The dihedral potential is of central importance in accurate descriptions of polymer properties. The difference in energy between rotational isomers such as trans and gauche states in alkanes determines the static stiffness and persistence length (statistical segment length σ). The height of the barriers between rotational isomeric states largely determines conformational dynamics and thereby strongly influences the monomeric friction ζ.[5] It is also well-known that torsional transitions are often correlated between neighboring dihedral degrees of freedom along a chain,[2,6−8] leading to the various cranklike motions.

Traditionally, experimental data on the relaxation behavior of short unentangled chains in the melt have been analyzed in terms of the Rouse model. This model describes the dynamic behavior of melt chains by a single-chain Langevin dynamics in which the other chains provide a background friction, ζ, and stochastic forces linked to the friction through the fluctuation−dissipation theorem. The model predicts properties such as the $1/N$ dependence of the center-of-mass diffusion coefficient referred to above. Experimental data[9] are generally corrected for the chain length dependence of the glass transition temperature in the melt—making the monomeric friction coefficient $\zeta(T,N)$ chain length dependent—by assuming the Rouse prediction for the center-of-mass diffusion coefficient to be correct. Computer simulations of an athermal system,[10] however, find a behavior $D \propto N^{-3/2}$ differing from the Rouse prediction.

On smaller length scales the internal relaxation of the melt chains can be studied by neutron spin−echo techniques. There it has been found that the Rouse model well describes poly(dimethylsiloxane) (PDMS) melts[11] but severely fails for polyisobutylene (PIB) melts.[12] Following an idea by Allegra and Ganazzoli,[13] this was rationalized as being due to the large difference in internal rotational barriers; PDMS has virtually no rotational barriers [$\Delta E \approx 100K$] whereas PIB has high barriers. Recently, a careful experimental study of PDMS and PIB chains of comparable chain structure has been performed.[14] The stiffness of both polymers as measured by the characteristic ratio is nearly identical, and chains of about the same chain length have been synthesized. This comparative study clearly showed that, for two polymers with the same meso- to large-scale chain structure, the dynamics of one (PDMS) was well described by the Rouse model whereas that of the other (PIB) was not, ruling out chain stiffness effects[15] as the reason for the failure of the Rouse model. The data on PIB could be well described by the Allegra and Ganazzoli model. However, the activation energy of the additional local time scale entering this model was not given by the internal rotational barriers of PIB as is implied in the construction of the model, but rather by a larger activation energy close to that of the structural relaxation.[12]

10.1021/ma0115794 CCC: $22.00
Published on Web 04/09/2002

This suggests that packing effects are playing a role, despite the very similar chain architecture of PDMS and PIB. In computer simulations we have the advantage that we can work with the same chemical polymer structure and simulate employing the full atomistic force field, and again, switching off all torsional potentials. In the case of polybutadiene this does not alter the meso- to large-scale chain structure, the same as in the experimental comparison of PDMS and PIB, but additionally we also keep the melt structure (packing) and density identical. For a short alkane oligomer (hexane) an analysis of the influence of the torsional barriers has been performed before,[16] but hexane is too short a molecule to display polymer specific effects.

In the next section we will give a few details on the simulation method. Section III will then discuss the results for the statics of our model systems, and section IV will discuss their chain dynamics. In section V we will present our conclusions.

II. Molecular Dynamics Simulations

We performed constant temperature NVT molecular dynamics (MD) simulations using three models for PBD. The first two models employ a validated[17] quantum chemistry based united atom potential that predicts the static[4,17] and dynamic[4,18,19] properties of a PBD melt in excellent agreement with experiment over a wide range of temperatures. For the first system, hereafter referred to as a chemically realistic chain (CRC1) model, the melt consists of 40 random copolymer chains, each with 30 repeat units having a 40% 1,4-cis/50% 1,4-trans/10% 1,2-vinyl microstructure. The second model, hereafter referred to as the CRC2 model, employed the same force field but without vinyl groups and used chains of 29 repeat units with a microstructure of 45% 1,4-cis units and 55% 1,4 trans units. The third model, hereafter referred to as the freely rotating chain model (FRC[20]), is the CRC2 model with all rotation potentials switched off.

We have looked at the high-temperature behavior of PBD melts and will discuss data obtained for temperatures between 273 and 353 K. (The glass transition temperature of this polymer is approximately 180 K.) Since the static properties of the CRC2 model and the FRC model are identical (see next section), we can use the latter for equilibration of the large-scale structure of the CRC2 melts and then perform a local equilibration switching on the dihedral potentials. Equilibration times ranged from about 10 ns for the CRC models at 353 K to about 100 ns for the FRC model at 273 K.[17]

III. Comparison of Static Properties

Let us begin by discussing the effects of switching off the dihedral potentials on the static properties of the models. In Figure 1 we show the population histograms for the β-dihedral (alkyl) and the α-dihedral (allyl) at the cis group.[17] In panel a two of the isomers for a typical alkyl torsion—the trans state at 180° and a gauche state at 60°—are visible for the CRC2 model. The distribution for the FRC model is almost flat, with a slight preference for the trans region due to the nonbonded interactions. The α-dihedral shows the skew state at 120° and a high population at the trans barrier (which is about 500 K). This effect has already been noted in the construction of RIS models for PBD.[17,21,22] Again, the FRC model shows the influence of intramolecular nonbonded interactions.

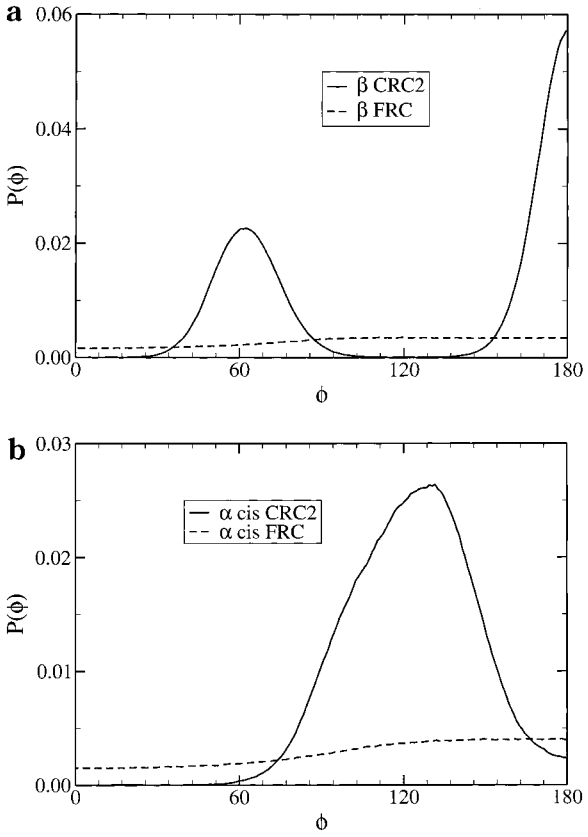

Figure 1. Comparison of the histograms of torsion angles observed in the simulation between the CRC2 and the FRC model at 273 K. Panel a is for the β dihedral (alkyl bond), and panel b is for the α-cis dihedral (allyl bond).

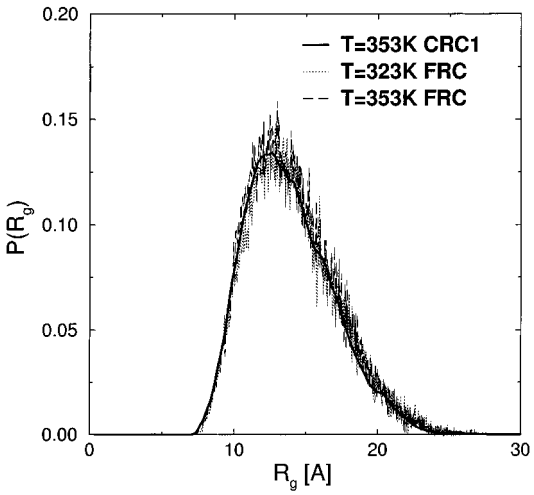

Figure 2. Probability distributions for the radii of gyration in the CRC1 at 353 K and the FRC model at 353 and 323 K.

When we now turn to the effect on the large-scale structure of the polymer, we observe that the distributions for the radius of gyration of the chains are completely identical between the models. Figure 2 shows them for the CRC1 model at 353 K and for the FRC model at 323 and 353 K. (The data for the FRC model are taken on a finer resolution and are therefore noisier.)

We will use the normal-mode analysis of the chain conformations to study the static and dynamical properties of PBD as predicted by the two models on scales from the statistical segment length to the size of the chain. For a melt chain exhibiting random walk statis-

tics on all length scales that conforms to the Rouse equation of motion,[23] the modes

$$\vec{X}_p(t) = \frac{1}{N}\sum_{n=1}^{N} \cos\left(\frac{\pi p(n - {}^1/_2)}{N}\right)\vec{r}_n(t) \qquad (1)$$

have the following autocorrelation function

$$\langle \vec{X}_p(t)\cdot\vec{X}_{p'}(0)\rangle = \delta_{pp'}\frac{\langle R_e^2\rangle}{8N(N-1)\sin^2\dfrac{p\pi}{2N}}\, e^{-p^2(t/\tau_R)} \qquad (2)$$

The squared amplitude of the first mode $\langle(\vec{X}_1(0))^2\rangle$ is connected to the end-to-end distance of the chain approximately as $\langle R_e^2\rangle/2\pi^2$ and the amplitudes of the larger modes are expected to scale as $\sin^{-2}(p\pi/2N)$. From the value of the characteristic ratio, $C_N \approx 5.2$, we expect to have $N_\sigma = 22$ statistical segments per chain. We will evaluate the Rouse modes up to $p = 40$.

For a real chain the Rouse modes are not exact eigenmodes. However, for the two models we study we find that the static cross-correlation amplitudes $\langle \vec{X}_p(0)\cdot \vec{X}_q(0)\rangle$, $q > p$, are zero within the statistical uncertainty of the simulation. (All recorded values are at most 2% of the diagonal values $q = p$.) The squared amplitudes of the first 40 modes are shown in Figure 3 for both models and several temperatures. Panel a shows that all data sets superimpose, and therefore both models have the same static structure on all length scales from below the statistical segment length up to the size of the chain. Furthermore, this structure does not depend on temperature for the depicted temperature range, which could be expected from the fact that the isomeric states are almost isoenergetic. However, the mode amplitudes follow the Gaussian $\sin^{-2}(p\pi/2N) \approx p^{-2}$ prediction only on the largest scale (the first two or three modes for polymer melts) and then cross over to an effective p^{-3} behavior as was observed earlier.[8,24] This crossover follows exactly an analytical prediction[26] for the normal mode amplitudes of a freely rotating chain. It could also be obtained by an approximation to a semiflexible chain model.[15] The agreement with the freely rotating chain calculation is shown in panel b where the amplitudes are plotted normalized to the value of the first mode. The mode amplitudes of the freely rotating chain can be written as

$$\langle \vec{X}_p^2(0)\rangle = \frac{\langle R_e^2\rangle}{8N(N-1)}\left[\frac{1}{\sin^2\left(\dfrac{p\pi}{2N}\right)} - \frac{1}{\gamma^2 + \sin^2\left(\dfrac{p\pi}{2N}\right)}(1 + O(N^{-1}))\right] \qquad (3)$$

where N is the number of united atoms and where we defined

$$\gamma^2 = \frac{(1 - |\langle\cos\theta\rangle|)^2}{4|\langle\cos\theta\rangle|} \qquad (4)$$

Equation 3 is valid for values $\cos\theta < 0$ of the mean cosine of the C−C−C bond angle. For $\langle\cos\theta\rangle = 0$ the second term in the square brackets is absent, and one recovers the Rouse result. The $O(N^{-1})$ term indicates a correction that is numerically unimportant for our chain length $N = 116$. The best fit value of $\langle\cos\theta\rangle = -0.7468$ differs from the value of -0.4843 directly observed in the simulation. Hence, also the model without dihedral potentials is not completely freely rotating due to residual nonbonded interactions preferencing the trans states of the dihedrals (see Figure 1). Nevertheless, the static structure of both models is well described by an effective freely rotating chain with the mean bond angle found in the fit.

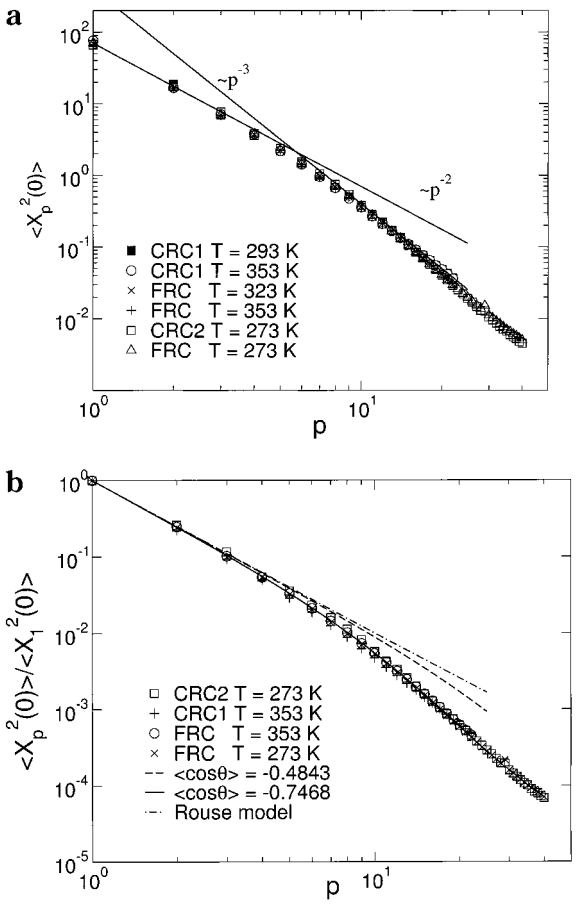

Figure 3. Mode dependence of the normal mode amplitudes for the CRC and FRC models at different temperatures. Panel a displays the unnormalized values showing that there is no observable temperature dependence in the structure of the chains and that the agreement between the CRC and FRC models holds over our complete temperature range. Panel b shows the amplitudes normalized by the $p = 1$ value to compare to the analytical predictions of the Rouse model and the freely rotating chain model. The FRC curves use the best fit value (−0.7468) for the cosine of the mean bond angle and the value observed in the simulation (−0.4843).

As a final result for the static structure, we want to look at the local packing in the melt. Figure 4 displays the static structure factor of the CRC2 and FRC melts calculated using only the united atom positions and equal scattering lengths for all united atom types. Both models show the same packing effects, and furthermore the position of the amorphous halo at $q \approx 1.45$ Å^{-1} is identical to the experimental findings.[25] Also, the position of the second peak around 3 Å^{-1} compares well with experiment. (The peak intensities cannot be compared since both experiment and simulation are given in arbitrary units.) To conclude this discussion on the static properties of the models, we have shown that local packing in the melt and chain structure from the scale of the statistical segment to the radius of gyration is identical for the CRC and FRC models.

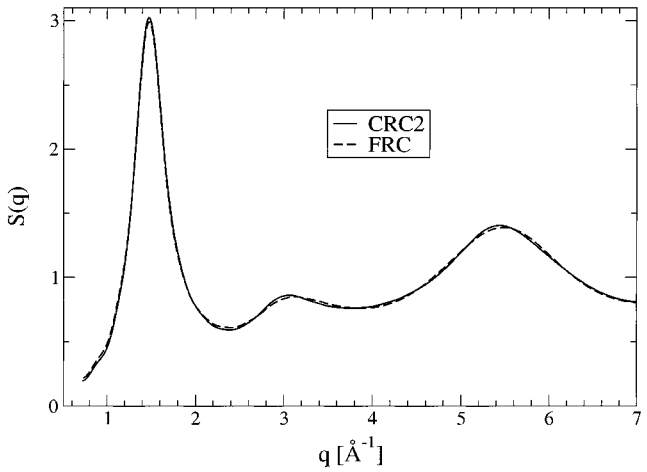

Figure 4. Static structure factor of the melt, comparing the CRC2 model (full curve and the FRC model (dashed curve). The position of the amorphous halo compares well with experimental data.

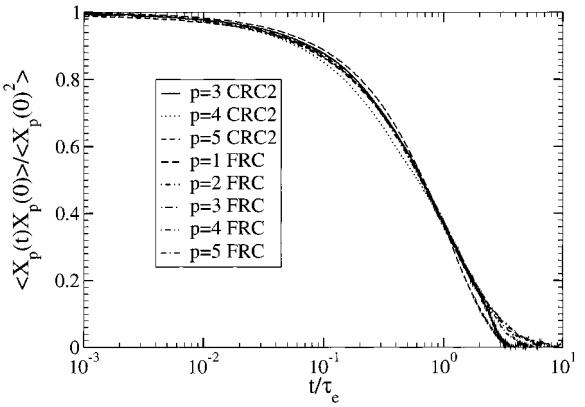

Figure 5. Comparison of the mode amplitude autocorrelation functions between the CRC2 model and the FRC model at 273 K. For each mode the time scale is normaliyzed by the 1/*e* decay time. For the CRC2 model modes $p = 1$, 2 do not decay sufficiently within our simulation time.

IV. Comparison of Chain Dynamics

For the computer simulation the chain dynamics is conveniently analyzed in terms of the Rouse modes. The dynamic autocorrelation function of the modes is known not to be describable by an exponential decay (eq 2) as derived in the Rouse model. It has been found for small mode numbers, $3 < p < 10$,[3,27] that their autocorrelation is better described by a stretched exponential Kohlrausch−Williams−Watts (KWW) function. In Figure 5 we compare the autocorrelation of the low-*p* Rouse modes between the FRC and the CRC2 models. All times are normalized to the 1/*e* decay time of the respective mode. The behavior is typical of that also found for coarse-grained models[24,28] and for polyethylene.[8] The first Rouse mode decays essentially exponentially, and the larger *p*, the stronger the stretching of the modes becomes. The range of modes displayed in Figure 5 is the one typically relevant for the description of NSE data on the dynamics of chains of the size we are studying.[29]

From this finding for the Rouse modes we can expect identical behavior for the single chain coherent intermediate scattering functions of the two models when the difference in overall mobility is scaled out. Figure 6 shows this function in comparison to the Rouse model prediction.[23] For the Rouse model calculation we need

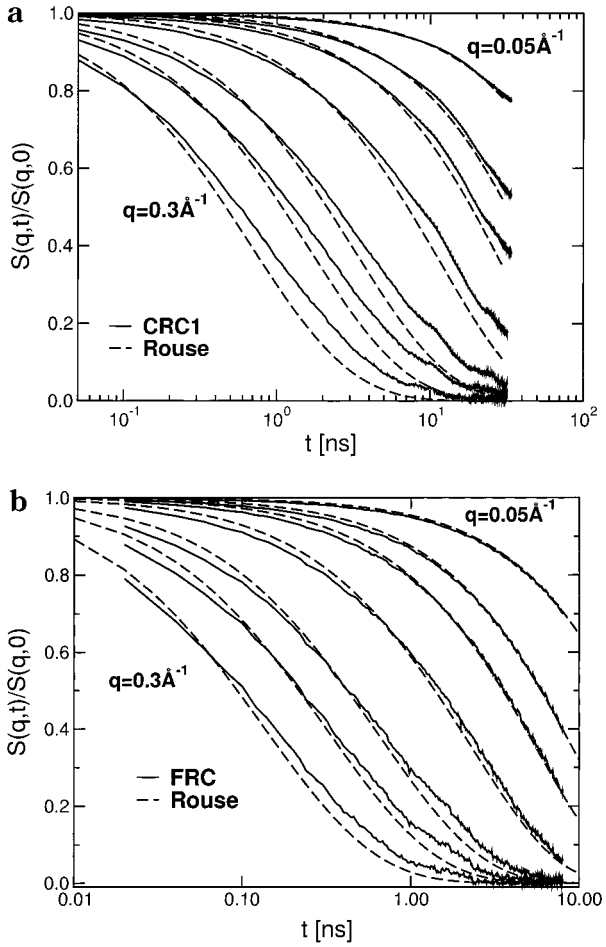

Figure 6. Comparison of the single-chain coherent intermediate scattering function as obtained from the simulation to the prediction of the Rouse model. Panel a is for the CRC1 model at 353 K, and panel b is for the FRC model at the same temperature.

the statistical segment length of the chains and the center-of-mass self-diffusion coefficient. These parameters can be determined independently in the simulation from the radius of gyration and the mean-squared center-of-mass displacement. As has already been discussed before,[19,27] the Rouse model prediction shows significant qualitative as well as quantitative deviations from the simulation data for the CRC1 model (see Figure 6a). Quantitatively, it overestimates the decay with increasing momentum transfer, and qualitatively it underestimates the stretching of the correlation functions. Since the CRC1 simulation data and the experimental data superimpose when plotted against diffusion coefficient times time[27]—thus scaling out an overall 20% difference in mobility between experiment and simulation—these conclusions hold for the experimental data as well. Figure 6b shows that the level of (dis)agreement with the Rouse model is comparable for the FRC model. For both models the behavior is intermediate between those found for PDMS and PIB experimentally.[14]

To quantitatively compare the CRC and FRC models, we plot their scattering functions vs scaled time in Figure 7. Of course, the FRC model is overall much more mobile and has a diffusion coefficient of $D = 17.24$ Å^2/ns at 353 K vs 3.12 Å^2/ns for the CRC1 model. In scaled time both sets of scattering curves superimpose, and therefore the models with and without torsional barriers

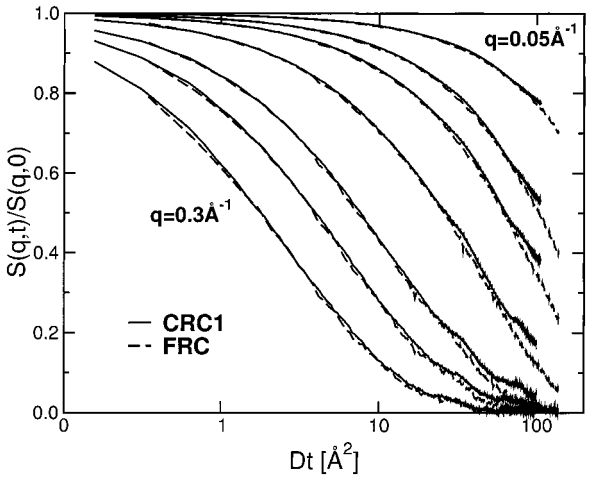

Figure 7. Single-chain coherent intermediate scattering function of the CRC1 model and FRC model plotted vs scaled time. The values of the center-of-mass diffusion coefficients of the chains are $D = 17.24$ Å^2/ns for the FRC model and $D = 3.12$ Å^2/ns for the CRC1 model.

have the same level of agreement or disagreement with the Rouse model in the typical range of momentum transfers studied in the NSE experiments.

V. Conclusions

We have presented MD simulations for two chemically realistic and a freely rotating chain model for PBD. On the basis of recent NSE experiments on PDMS and PIB, it has been suggested that the agreement between experiment and the Rouse model prediction for the single-chain coherent intermediate scattering function should be much better for chains with low internal rotation barriers than for chains with high barriers. For our CRC and FRC models we showed that their melt structure factor (local packing) and the meso- to large-scale chain structure are completely identical. In this situation, our simulations show that the level of agreement with the Rouse model for the meso- to large-scale chain dynamics, i.e., the range of momentum transfer studied in NSE experiments, does not depend on the presence of rotational barriers. The scattering functions of the chemically realistic models and the freely rotating model are identical when time is rescaled by the respective chain center-of-mass diffusion coefficient, and both disagree with the Rouse model description. Therefore, even the total absence of torsional barriers does not guarantee that the Rouse model is able to account for the scattering data.

On the other hand, we have shown before[19] that the Rouse model prediction for the chain coherent scattering of PBD agrees with a calculation of the scattering from the simulation which is done using the dynamic Gaussian approximation, i.e., when it is assumed that the atom displacement distribution is Gaussian at all times. This indicates that the failure of the Rouse model is due to its inability to describe non-Gaussian displacement behavior. The most obvious contradiction to the dynamic Gaussian assumption is observed in the subdiffusive center-of-mass motion of the chains on time scales below the Rouse time.[19,27] This subdiffusive motion can only be caused by interchain interactions.

In the Rouse model both intra- and intermolecular effects on the mobility are summarily taken into account by just one parameter, the monomeric friction coefficient, ζ. It is puzzling that for PDMS melts and solutions[14] this crude single-chain approximation is obviously sufficient to yield a good quantitative description of the chain diffusion as well as the intramolecular relaxation on length scales on which the chains can be treated as Gaussian coils. For other polymers, like PIB in the melt and in solution[14] or PBD examined in this work the Rouse approximation breaks down. The analysis in refs 12 and 14 suggests to improve the theoretical description through the phenomenological ansatz of Allegra and Ganazzoli introducing a second independent dissipation mechanism being interpreted as due to intramolecular rotation barriers.

An analysis of neutron scattering data on PIB solutions gave an activation energy of about 3 kcal/mol[14] for this additional mechanism, and for PIB melts 10 kcal/mol[12] was obtained. Both values disagree with the best estimate for the effective intramolecular rotation barrier for the trans−gauche transition in PIB of 5 kcal/mol obtained theoretically,[30] seen in simulations of PIB melts[31] and also in NMR experiments on PIB solutions.[32] From the simulations[31] one can also directly access the rate for conformational trans−gauche transitions. The temperature dependence of this quantity in the melt yields an activation energy of 7.4 kcal/mol, which is larger than the effective rotation barrier of 5 kcal/mol showing an influence of the local packing on the barrier transitions. The additional dissipation mechanism captured in the fit with the Allegra model therefore seems to be different in PIB solutions and melts and not quantitatively linked with the intramolecular barriers.

Combining these findings and our results presented in this work, we conclude that the phenomenological introduction of an additional dissipation mechanism into a Rouse-like single-chain theory of polymer melt dynamics improves its ability to fit experimental scattering data but does not lead to an easily identifiable physical process underlying this mechanism. The latter difficulty originates from the attempt to capture many-particle effects in an effective single-particle theory. The presence of internal rotational barriers as the only reason for deviations from Rouse-like behavior can be ruled out.

Acknowledgment. W.P. and S.K. acknowledge support through the German Science Foundation under Grant PA 473/3-1,2 and the BMBF under Grant 03N6015. G.D.S acknowledges support from the American Chemical Society PRF program through Grant 67-301 and from the Sonderforschungsbereich 262 for a stay in Mainz.

References and Notes

(1) Binder, K., Ed.; *Monte Carlo and Molecular Dynamics Simulations in Polymer Science*; Oxford University Press: Oxford, 1995.
(2) Smith, G. D.; Yoon, Do Y.; Zhu, W.; Ediger, M. D. *Macromolecules* **1994**, *27*, 5563.
(3) Paul, W.; Smith, G. D.; Yoon, Do Y.; Farago, B.; Rathgeber, S.; Zirkel, A.; Willner, L.; Richter, D. *Phys. Rev. Lett.* **1998**, *80*, 2346.
(4) Smith, G. D.; Paul, W.; Monkenbusch, M.; Willner, L.; Richter, D.; Qiu, X. H.; Ediger, M. D. *Macromolecules* **1999**, *32*, 8857.
(5) Paul, W.; Yoon, Do Y.; Smith, G. D. *J. Chem. Phys.* **1995**, *103*, 1702.
(6) Helfand, E.; Wassermann, Z. R.; Weber, T. A. *J. Chem. Phys.* **1979**, *70*, 2016.
(7) Boyd, R. H.; Gee, R. H.; Han, J.; Jin, Y. *J. Chem. Phys.* **1994**, *101*, 788.

(8) Paul, W.; Smith, G. D.; Yoon, Do Y. *Macromolecules* **1997**, *30*, 7772.
(9) Pearson, D. S.; Fetters, L. J.; Graessley, W. W.; Ver Strate, G.; von Meerwall, E. *Macromolecules* **1994**, *27*, 711.
(10) Müller, M.; Wittmer, J.; Barrat, J. L. *Europhys. Lett.* **2000**, *52*, 406.
(11) Richter, A.; Ewen, B.; Farago, B.; Wagner, T. *Phys. Rev. Lett.* **1989**, *62*, 2140.
(12) Richter, D.; Monkenbusch, M.; Allgeier, J.; Arbe, A.; Colmenero, J.; Farago, B.; Cheol Bae, Y.; Faust, R. *J. Chem. Phys.* **1999**, *111*, 6107.
(13) Allegra, G.; Ganazzoli, F. *Macromolecules* **1984**, *14*, 1110; *Adv. Phys. Chem.* **1989**, *75*, 265.
(14) Arbe, A.; Monkenbusch, M.; Stellbrink, J.; Richter, D.; Farago, B.; Almdal, K.; Faust, R. *Macromolecules* **2001**, *34*, 1281.
(15) Harnau, L.; Winkler, R. G.; Reineker, P. *J. Chem. Phys.* **1995**, *102*, 7750.
(16) Travis, K. P.; Brown, D.; Clarke, J. H. R. *J. Chem. Phys.* **1995**, *102*, 2174.
(17) Smith, G. D.; Paul, W. *J. Phys. Chem. A* **1998**, *102*, 1200.
(18) Smith, G. D.; Borodin, O.; Bedrov, D.; Paul, W.; Qiu, X. H.; Ediger, M. D. *Macromolecules* **2001**, *34*, 5192.
(19) Smith, G. D.; Paul, W.; Monkenbusch, M.; Richter, D. *J. Chem. Phys.* **2001**, *114*, 4285.
(20) Flory, P. *Statistical Mechanics of Chain Molecules*; Hanser: Munich, 1988.
(21) Abe, Y.; Flory, P. J. *Macromolecules* **1971**, *4*, 219.
(22) Mark, J. E. *J. Am. Chem. Soc.* **1966**, *88*, 4354; **1967**, *89*, 6829.
(23) Doi, M.; Edwards, S. F. *The Theory of Polymer Dynamics*; Clarendon Press: Oxford, 1986.
(24) Kopf, A.; Dünweg, B.; Paul, W. *J. Chem. Phys.* **1997**, *107*, 6945.
(25) Richter, D.; Frick, B.; Farago, B. *Phys. Rev. Lett.* **1988**, *61*, 2465.
(26) Kreer, T.; Baschnagel, J.; Müller, M.; Binder, K. *Macromolecules* **2001**, *34*, 1105.
(27) Smith, G. D.; Paul, W.; Monkenbusch, M.; Richter, D. *Chem. Phys.* **2000**, *261*, 61.
(28) Okun, K.; Wolfgardt, M.; Baschnagel, J.; Binder, K. *Macromolecules* **1997**, *30*, 3075.
(29) Richter, D.; Willner, L.; Zirkel, A.; Farago, B.; Fetters, L. J.; Juang, J. S. *Macromolecules* **1994**, *27*, 7437.
(30) Boyd, R.; Breitling, S. *Macromolecules* **1972**, *5*, 1.
(31) Karatasos, K.; Saija, F.; Ryckaert, J.-P. *Physica B* **2001**, *301*, 119.
(32) Dejean de la Batie, R.; Lauprêtre, F.; Monnerie, L. *Macromolecules* **1989**, *22*, 2617.

MA0115794